Experimental Study and Numerical Analysis on Effect of Opening with Different Aspect Ratio in Squat Wall

By

Arbaz khan

Registration No -329394

Thesis Supervisor Dr. Azam Khan

Department of

Structural Engineering

National Institute of Civil Engineering (NICE)
School of Civil and Environmental Engineering (SCEE)
National University of Sciences & Technology (NUST)
Islamabad, Pakistan

2023

Experimental study and numerical analysis on effect of opening with different aspect ratio in squat wall

Author

Arbaz khan

Regn Number

329394

A thesis submitted in partial fulfillment of the requirements for the degree of

MS Structural Engineering

Thesis Supervisor:

Dr. Azam Khan

Thesis Supervisor's Signature:

_____

Department of Structural Engineering

National Institute of Civil Engineering (NICE)

School of Civil and Environmental Engineering (SCEE)
National University of Sciences & Technology (NUST)
Islamabad, Pakistan

June 2023

Declaration

I certify that this research work titled "*Experimental study and numerical analysis on effect of opening with different aspect ratio in squat wall"* is my own work. The work has not been presented elsewhere for assessment. The material that has been used from other sources it has been properly acknowledged / referred.

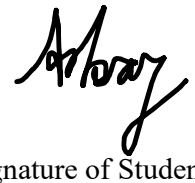

Signature of Student

Arbaz khan

2023-NUST-Ms-Structural Engineering-329394

Copyright Statement

THESIS ACCEPTANCE CERTIFICATE

It is certified that final copy of MS thesis written by Mr. Arbaz khan, Registration No. 00000329394, of MS Structural Engineering batch 2020 (NICE), has been vetted by undersigned, found completed in all respects as per NUST Statutes/Regulations, is free of plagiarism, errors, and mistakes and is accepted as partial fulfilment for award of MS degree.

Signature: _____

Supervisor: Dr. Azam khan

Date: 20/07/23

HoD Structural Engineering
NUST Institute of Civil Engineering
School of Civil & Environmental Engineering
National University of Sciences and Technology

Signature (HoD): _____

(Dr. Muhammad Usman)

Date: 20-7-23

Signature (Principal & Dean): _____

PROF DR MUHAMMAD IRFAN
Principal & Dean
SCEE, NUST

Date: 21 JUL 2023

ACKNOWLEDGEMENT

"**In the name of Allah, the most beneficent the most merciful**"

Foremost, I would like to express my earnest thankfulness to my supervisor Dr. Azam Khan for his persistence, interest, and massive knowledge. His guidance helped me in all the time of research and writing this thesis. His pleasing and welcoming behavior facilitated me to discuss my point ofview on the topic in detail and resolved my queries to my full satisfaction.

Here, it is worth mentioning that the completion of this study was possible due to the assistance ofmany dedicated and helpful colleagues. In addition to my supervisor and committee members, I am also thankful to my friends, specially Syed Aqeel Shah for supporting me all the way through my study.

Finally, I extend my profound gratitude to my family members, for all that they meant to me throughout this critical time of completion of my study.

Abstract

The center of attention of this research is to study the effect of window opening with different aspect ratio on in plane shear capacity of RCC-squat wall both experimentally and numerically. For this goal three scaled models of squat wall have been casted have opening of same area but with different aspect ratio in each wall. Opening having B/H ratio of 1/2, 1 and 2/1 were used. The opening area was 10% of wall area. All three samples were tested under monotonic loading with the same loading rate. The experimental measure was the in-plane force and horizontal displacement. It has been found that wall having opening aspect ratio of B/H=1/2 gives highest in plane share capacity while wall having opening, with B/H=2/1 gives least capacity and is more detrimental to shear capacity. In last numerical model has been developed using ABAQUS Software as a FEM package to numerically validate our experimental results. The finite element simulation was carried out as per suggested modelling techniques and by comparison with experimental result the credibility of numerical model has been checked. This result of numerical was found very close to experimental results. This study now provides a strong base for selecting opening aspect ratio either in already constructed squat wall and in newly designed squat wall.

Key Words: Monotonic loading, Forced response analysis, Numerical analysis, Squat wall, shear wall

Chapter-1

Chapter-2

Chapter-3

Chapter-4

Chapter-5

Chapter-6

List of Tables

List of Figures

Chapter-1

1 Introduction:

1.1 General:

When creating a structure, a shear wall is a structural component used to withstand lateral forces including wind loads and seismic forces. In order to give strength, stiffness, and stability within a building, it is often a vertical wall consisting of reinforced concrete, masonry, or steel that is positioned in a strategic location[1].

A building's lateral stresses are transferred from the shear wall to the foundation, which reduces the building's lateral deflection and prevents excessive swaying during intense occurrences. Shear walls assist in preserving the overall stability and integrity of the building by fending against these lateral forces.[1]

Shear walls function via the shear resistance mechanism. These walls experience shearing stresses when lateral forces are applied to a structure. These shear pressures are resisted by the reinforcing bars that are included into the concrete or steel that makes up the shear wall. Its capacity to bear these forces is a result of the wall's shape, material characteristics, and reinforcement details.[2]

Shear walls must be designed considering factors including their position, orientation, thickness, aspect ratio, and reinforcing detailing. To guarantee that the shear walls can withstand lateral stresses and distribute them to the foundation, proper design and details are essential.[3]

Shear wall design and construction parameters are provided by several codes and design guides, such as the American Concrete Institute (ACI) 318. These recommendations assist engineers in determining the proper reinforcement scheme, dimensions, and connections required to achieve the specified structural performance. In general, shear walls are crucial parts of building design, especially in regions vulnerable to strong winds or seismic activity. They are essential in preventing lateral loads from being imposed on structures while also improving their overall stability and safety.[1]

Squat walls are a form of reinforced concrete shear wall having a small height relative to its length. They are also known as short or low aspect ratio shear walls. It usually has a height to length ratio (Aspect Ratio) of less than or equal to 1.5. Especially in seismic areas, squat walls are frequently utilised in building design to provide lateral load resistance and improve structural stability. Squat walls can successfully withstand lateral stresses like those caused by earthquakes or wind loads despite their shorter height. They typically show modest flexural (bending) behaviour and a mostly shear response.[4]

Squat walls must be designed with factors including placement, orientation, thickness, reinforcing details, and aspect ratio in mind. Squat walls must be properly designed and detailed in order to efficiently withstand lateral stresses and transfer them to the foundation.

For the design and construction of squat walls, requirements and suggestions are provided by design codes and guidelines such the American Concrete Institute (ACI) 318.[1]

Studies have been carried out to better understand the behaviour and design of squat walls. These studies concentrate on elements including the placement of the reinforcement, the implications of the aspect ratio, boundary conditions, and performance under various loading scenarios. They want to improve people's knowledge of and ability to use squat walls in structural systems.

Openings such as windows, doors, or architectural details may occasionally be included into shear walls in building design for reasons other than structural ones. These apertures fulfil architectural requirements by supplying the building with light, ventilation, or aesthetic appeal. It's crucial to understand that these gaps might end up being possible weak spots in the shear walls' structural performance.[6]

Shear walls are primarily made to withstand lateral forces and give the structure structural stability. They depend on their ability to convey these lateral loads to the foundation without interruption since they are continuous. Shear walls' continuity and integrity are jeopardized when openings are made in them, which can affect how well they support structures.[2]

Shear wall apertures can cause stress to concentrate near the openings' edges and alter the load path. The shear wall's strength and stiffness may be diminished at and around the openings because of this concentration of forces. Openings diminish the shear wall's resistance to lateral stresses as a result, which might jeopardize the structure's overall stability.[7]

Openings in shear walls are prohibited by building design standards and recommendations to reduce the possible detrimental impacts of openings. To maintain the structural integrity of the wall, these measures frequently call for extra reinforcement or particular detailing around the apertures. For instance, according to design regulations like the American Concrete Institute (ACI) 318, steel bar reinforcements that are cut off to provide openings may need to be terminated with seismic hooks or capped with U-shaped bars.

The effect of apertures on shear walls must be carefully considered by structural engineers, architects, and builders, who must also adhere to the specifications and norms set out in the pertinent design regulations. By doing this, they may assure that the non-structural design goals are met without compromising the shear walls' structural performance. [8,9]

Squat walls made of reinforced concrete are vertical elements that transfer vertical loads from a building's diagram to its foundation. The ratio of their height to length determines how they fail. (Cyclic Behaviour of Square Reinforced Concrete Shear Walls Enhanced with Fiber-Reinforced Polymer). Opening statements by Alaa Aly El-Sayed, Mohamed Sayed Goma, and Mostafa Mamdouh Mohamed)[10]

The RC squat wall with opening has just undergone the first experimental and analytical study. [11]

The impact of these apertures on the nonlinear performance of shear walls has drawn more attention since the presence of gaps in RC shear walls becomes inevitable in many situations owing to architectural or mechanical reasons. Most studies that looked at the impact of apertures on the behaviour of RC shear walls have lately looked into reinforcing these walls

using openings. Because mechanical and architectural factors might sometimes make it necessary to provide openings in squat walls.[13,14]

Sotomura et al. have researched the behaviour of shear walls with many openings in pipes and ducts in PWR nuclear power plants. Diagonal reinforcement has been used to assure the strength and stiffness of the shear wall with these apertures in a significant number of openings. 11 shear wall specimens with holes that had various reinforcing designs were tested by Lin and Kuo. It has been discovered that shear strength is significantly impacted by reinforcing around openings. In RC walls, the impact of staggered door openings has already been researched by Ali and Wight. Yanez et al. investigated six rectangular walls with irregular openings, and they discovered that staggered apertures exhibit comparable ductility and behaviour to that of normal ones.

1.2 Previous Model:

Several empirical and semi empirical equations have been presented by code and literature to calculate shear capacity of RC shear wall without opening.

Starting with ACI-318-19, the in-plane shear capacity of squat wall can be computed by using following relations,

The contribution from concrete is

$$V_C = A_g \alpha \lambda \sqrt{f'}$$

Whear as the contribution from steel is

$$V_S = A_g \rho_t f_y$$

Total shear capacity is the summation of contribution from concrete and steel.

$$Vn = Vc + Vs$$

ASCE/SEI present following equations for calculating shear capacity of shear wall.

$$Vc = \left[8.3\sqrt{f'c} - 3.4\sqrt{f'}\left[\frac{h_w}{l_\omega} - 0.5\right] + \frac{N_v}{4lwtw}\right] t_w d.$$

Whear VC is contribution from concrete and that VS is from steel.

$$V_s = \rho_{se} f_y t_\omega d$$

Likewise IS 456:2000 estimate horizontal capacity subjected to non-seismic loads by using following relation,

$$If\ {h_w}/{l_\omega} \le 1$$

$$v_c = \left[\left[3 - {h_\omega}/{h}\right] k_1 \sqrt{f_{ck}}\right](0 \cdot 8 l_\omega t_w) \ge k_3\ \sqrt{f_c}(0 \cdot 8 l_\omega t_\omega)$$

$$If\ {h_w}/{l_\omega} \ge 1$$

$$v_c = \left[k_2 \sqrt{f_{ck}} \frac{\left[\frac{h_\omega}{l_\omega} + 1\right]}{\left[\frac{h_w}{l_w} - 1\right]}\right](0 \cdot 8 l_\omega t_w) \ge k_3\ \sqrt{f_c}(0 \cdot 8 l_\omega t_\omega)$$

Some researchers have also proposed equations to calculate shear capacity for walls as follow [14-19]. A semi empirical equation by EIJ for estimating horizontal shear capacity for wall subjected to seismic loading as

$$V = \frac{tan\ tan\ \theta(1-\beta) t L \vartheta f_c'}{2} \ge 0$$

Where $v = 0.7 - (f_c'\ /\ 2000)$; $tan\ \theta = \sqrt{\left({h_w}/{I_w}\right)^2 - 1} - {h\omega}/{l_\omega}$;

$$\beta = (1 + cot^2\ \varepsilon)\rho_h f_y\ /\ vf'$$

Contribution to shear strength from steel is

$$V_S = \rho_h f_y l_\omega t_\omega$$

vAn empirical equation suggested by Sanchez-Alejandre and Alcocer based up strut and tie model for shear strength of wall is following.

$$v_S = v_c + v_S$$

Contribution of shear strength from concrete is

$$v = \left[\gamma \eta_v + \frac{0.04 N_u}{A_\omega}\right] \sqrt{f_C'}$$

While that from steel is

$$v_s = \eta_h p_v f_y$$

All of the aforementioned equations predict a squat wall's shear capacity in the absence of an aperture, but when one is present, the squat wall's shear capacity drops sharply. According to a study on the strength and behaviour of reinforced concrete squat shear walls with openings under cyclic loading, the drop might occasionally even reach 40%, which is a significant amount. Therefore, thorough study on this subject is essential in today's world. A significant amount of study has previously been done on the subject, as many researchers have recently attempted to do. V. Sivaguru and G. Appa Rao's study has led to the modification of the ACI-formula that is described below.

$$v_n = \left(\alpha_C \lambda \sqrt{f'} + \rho_t f_{yt}\right)\left(A_{Cv,left} + A_{Cv,right}\right)$$

(Shear behaviours of reinforced concrete structural walls with eccentric apertures under cyclic loading: experimental research) Due to architectural requirements, the opening area is of various forms and sizes.

Even though there has been a lot of study on the behaviour of squat walls with openings over the last few decades (Nishiyama and Ono, 1995; Qamaruddin, 1998; Lopes, 2001), it still isn't adequate to fully explain the behaviour. Shear strength is depending on the position of the opening relative to the application of stress, according to Jiyang Wang et al. As previously said, even though a significant amount of study has already been done on the opening in squat walls, it is still unclear how the aspect ratio of the aperture affects the shear capacity of shear walls, particularly squat walls. This study has been done out

1.3 Research Significance

The behaviour of reinforced concrete (RC) squat shear walls with apertures is not well understood in its entirety. The size and placement of the apertures have a significant impact on the seismic response of these walls. Research that focuses on understanding the behaviour of and developing strengthening methods for walls with apertures is therefore essential. As a result, focused research efforts are required in this area. By providing a numerical analysis of shear walls with apertures, this paper seeks to add to the body of current knowledge.

Chapter-2

2 Experimental Procedure:

Three one-third sized models were built in order to examine the performance of squat walls with various aspect ratio apertures. A squat wall with a varied aspect ratio opening was portrayed by each model. To meet the minimal requirements outlined in the IBC-2000 code, the apertures were created with an area equivalent to 10% of the total wall area.

The experiment's apertures had aspect ratios of 2:1, 1:1, and 1:2 (Figure 1). This indicates that the apertures' breadth varied in relation to their height. To find out how the size and proportions of the apertures affect how well squat walls function, several aspect ratios were used.

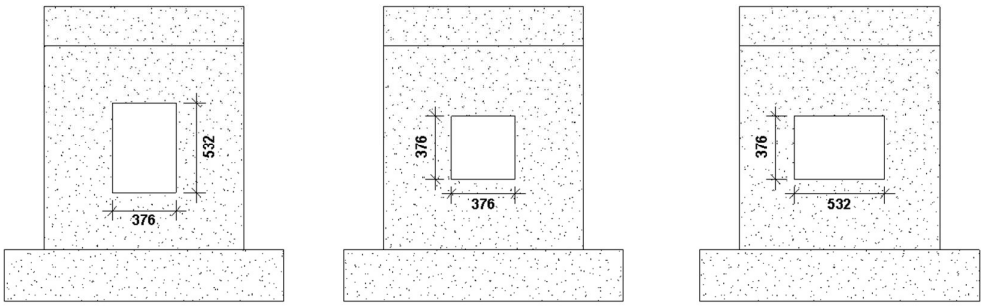

Figure 1: Opening Sizes

The displacement at the top of each wall was monitored during the experiment. This measurement gave information on the wall's deformation characteristics and assisted in assessing how the wall responded to the imposed load.

To maintain uniformity and remove any variances in material qualities, it is important to note that all the walls were cast from the same batch of materials. This method made it possible to compare the effectiveness of squat walls with various aspect ratio apertures in a fair and precise manner Table 1.

The study aims to evaluate the impact of the aspect ratio of openings on the performance of squat walls by comparing the data obtained from each wall. The results would be helpful in understanding how squat walls with various opening configurations behave and react structurally.

Each specimen's top beam was subjected to load in the experimental setting. The wall finally collapsed as the strain progressively rose. This monotonic loading strategy made it possible to observe how the wall behaved and performed as applied stresses increased.

S No.	Sample	Length	Hight	Thickness	Opening Height	Opening Width	concrete Compressive strength	Steel

1	Wall 1:2	1180	1200	100	540	266	21	275
2	Wall 1:1	1180	1200	100	376	376	21	275
3	Wall 2:1	1180	1200	100	266	540	21	275

Table 1: Specimen Parameter and Material Properites

In the experimental investigation, squat walls were intended by designing all three walls to have the same exterior dimensions. This was accomplished by keeping the length to breadth ratio of each wall close to 1, which made the walls seem squat and comparatively short. All three specimens had a typical thickness of 100mm.

It was crucial to keep the reinforcement ratios of the walls constant in order to focus the investigation on the impact of apertures. For all three examples, the horizontal and vertical reinforcement ratios were constant. This indicates that the reinforcement's quantity and distribution within the walls were both the same.

Each wall opening's total area was reported as being 141600 mm2. The apertures' size and form differed, nonetheless, amongst species. The hole in specimen S2 was square and measured 376 mm by 376 mm. The aperture in specimen S1 was rectangular and measured 532 mm by 266 mm. The hole in specimen S3 measured 266mm by 532mm and had the same size but a different orientation. For specimen S3, this led to a height-to-width ratio of 0.5.

The study tried to isolate the effect of the openings on the performance of the squat walls by maintaining the reinforcement ratios and exterior dimensions while changing the aspect ratios and orientations of the apertures. This method made it possible to investigate in greater detail how various aspect ratios and opening configurations impact the structural performance and responsiveness of the walls to applied loads.

9mm diameter bars were utilised in each specimen to strengthen the web of the wall. These bars were evenly placed, both horizontally and vertically, at 100mm intervals. The wall's strength and structural integrity are improved by the reinforcement, enabling it to bear the imposed stresses.

A 200mm x 200mm beam was cast on each web to mimic a more robust link between the wall and the slab and prevent stress accumulation at the point where the load is applied. The purpose of this beam is to more equally distribute the weight along the wall and lessen the possibility of localised stress concentration.

The top beam of each specimen was strengthened with four longitudinal bars that were 12mm in diameter in addition to the reinforcement in the web. These bars give the top of the wall—which is frequently under greater stress during load application—additional strength and rigidity.

Stirrups were used as shear reinforcement to guarantee acceptable shear resistance. These stirrups were spaced out at regular intervals of 100mm and had a diameter of 9mm. The stirrups' main function is to withstand internal shear stresses and guard against shear failure.

The webs of all three examples were cast monolithically with the foundation in order to stabilise the walls and secure them during the application of lateral loads. Eight 12mm-diameter bars that were placed throughout the foundation's length to provide longitudinal reinforcement. To increase the foundation's shear strength, shear rings were added to it that were made of 9mm bars spaced 200mm apart.

This reinforcing arrangement, taken together, makes sure that the squat walls are strong and rigid enough to bear the imposed lateral stresses, distribute them efficiently, and preserve stability. The web, top beam, and foundation all contain reinforcement, which improves the walls' structural performance and lowers their failure risk.

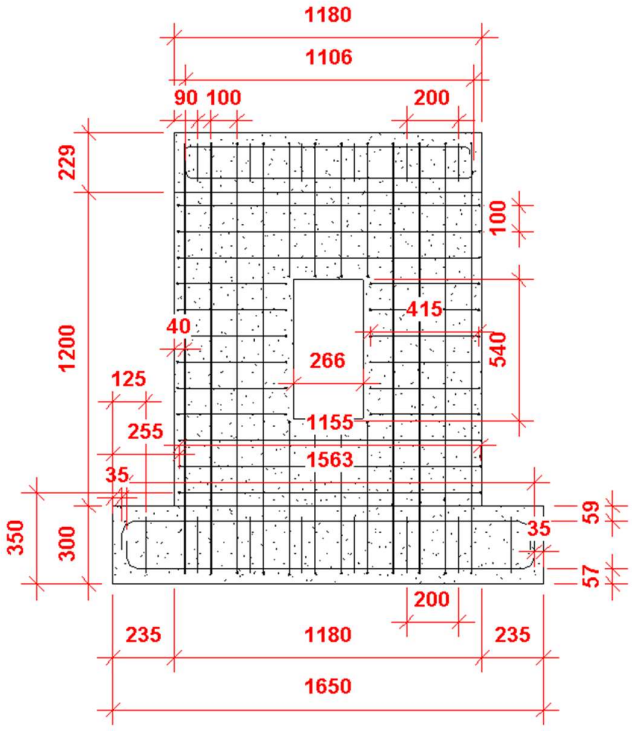

Figure 2: Reinforcement Detail Elevation

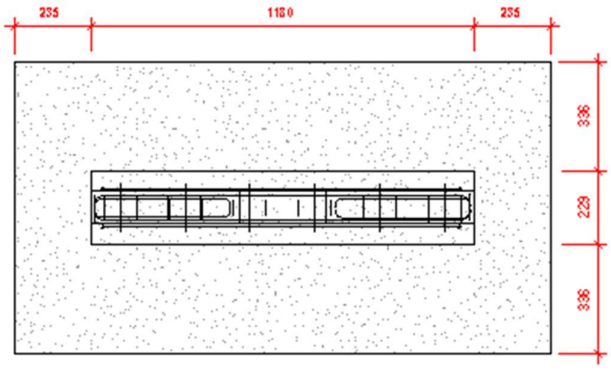

Figure 3: Reinforcement Detail Plan View

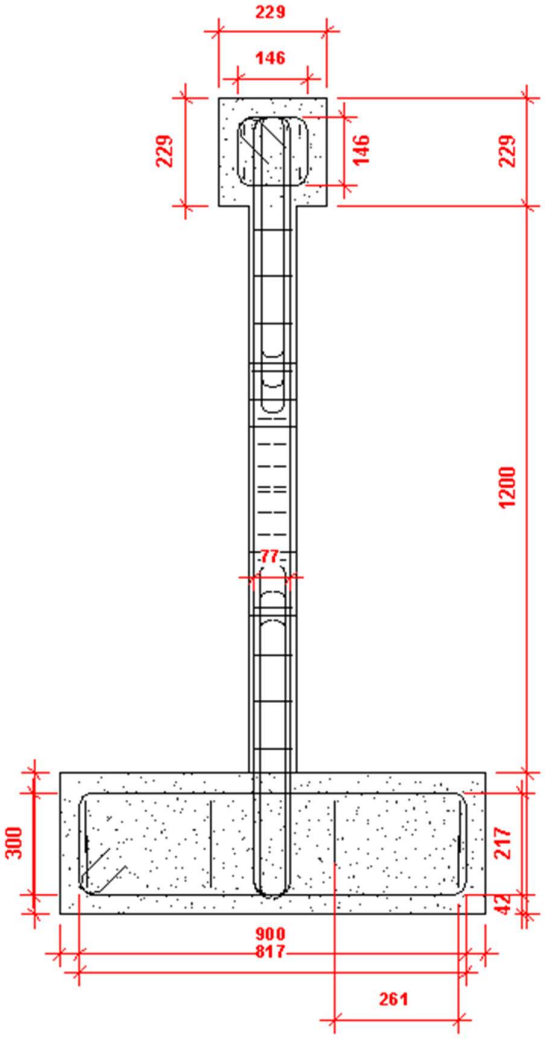

Figure 4: Reinforcement Detail Side View

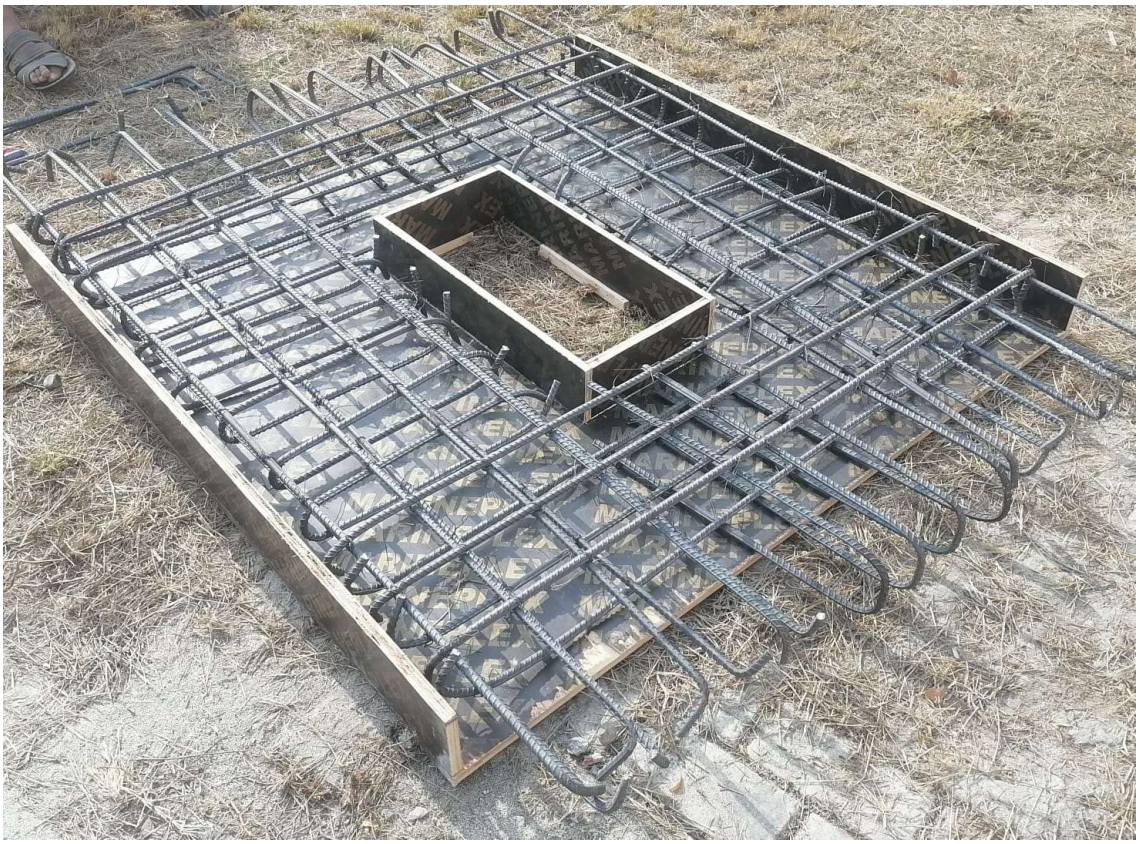

Figure 5: Web Reinforcement for Wall 1:2

2.1 Testing Rig and gauge arrangement:

For each of the three walls, the experimental setup was the same. As shown in Figure **, a jack was placed on the top beam of each wall to apply the weight. The response frame, which was situated on the rear side of the wall, was linked to the jack. Each beam's top was fitted with a load cell utilising an assembly in order to measure the applied load.

Using a linear variable differential transformer (LVDT), the top beam's movement was observed. To precisely measure the movement of the beam, the LVDT was carefully positioned. A data logger was attached to both the load cell and the LVDT, allowing the synchronisation of the recorded results in the time domain.

In conclusion, a jack was used to apply the load to the top beam, and a load cell and LVDT were used to measure the applied load and the displacement of the beam, respectively. A data logger was used to capture and synchronise these readings for further study.

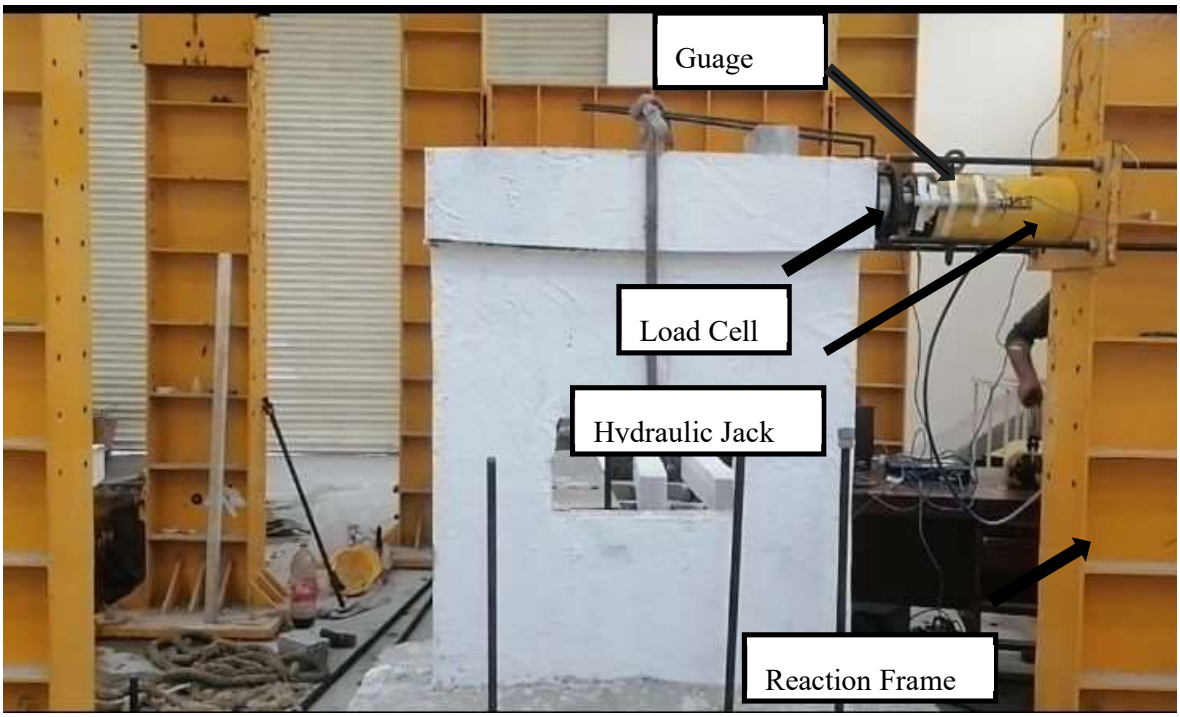

Figure 6: Experimental Setup

Eight two-inch-diameter bolts were used to firmly fasten the foundation to a hard floor in order to maintain stability and prevent the wall from moving. During the experimental testing, this anchoring technique successfully immobilised the foundation and stopped any unintended movement or rotation of the wall. It was also critical to prevent any unintentional out-of-plane incidents on the wall. The possibility of any unintentional twisting or tilting of the specimen was reduced by properly transmitting the lateral stress imparted to the wall via the foundation by firmly fastening it to the rigid floor.

During the experimental testing, a hydraulic jack with a 100-ton capacity was used to apply the load. For precise measurements of the structural reaction and behaviour, the hydraulic jack applied the load to the top beam of the wall in a controlled and progressive manner. The experimental setup assured the stability, safety, and controlled loading of the wall specimens during testing by putting these precautions in place, including the secure attachment of the foundation to the firm floor and the use of an adequate hydraulic jack.

The structural laboratory at Semnan University was used for all of the preparation, equipment setup, and specimen testing. Following the casting procedure, each specimen was properly kept in an environment with a relative humidity of 40% and an ambient temperature of around 26 °C. The specimens were demolded after a day and tightly packed in plastic bags to preserve their moisture content.

The specimens had no holes when they were first being cast. The wall webs were purposefully sliced using a concrete saw to make the necessary apertures after 35 days from the time of

casting. This made it possible to carefully and precisely insert apertures in the samples for additional testing and analysis.

Figure 7: Wall Web With Opening of Different Aspect Ratio

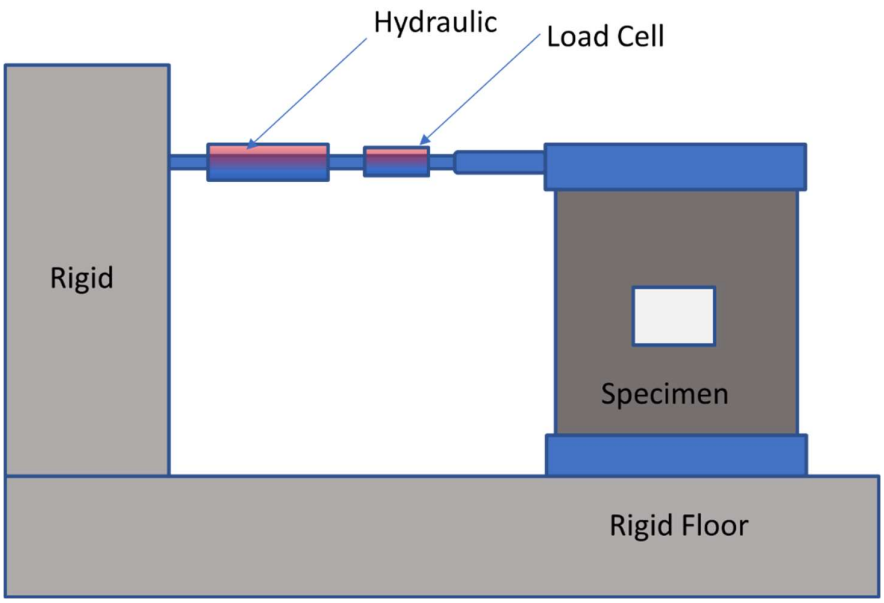

Figure 8: Skematic Diagram of Testing Setup

2.2 Material properties:

A typical concrete mix with a water to cement ratio of 0.43 was utilised to build the RC shear walls. The compressive strength of this mixture was intended to be around 20 MPa. To guarantee compliance with the distance between the steel bars and the mold's specifications, a maximum aggregate size of 25 mm was chosen.

Three cylindrical specimens with dimensions of 150 mm in diameter and 300 mm in height were created to test the concrete's compressive strength. Compressive stresses were applied to these specimens at a rate of 1.8 mm per minute. The concrete's compressive strength was assessed after 28 days. After 28 days, the compressive strength was around 21 MPa on average (individual readings ranged from 20.2 to 20.7 MPa).

Two different kinds of steel bars—D12 and D16—were used to strengthen the RC shear walls. Experimental testing was used to establish the diameter and other features of these steel bars' mechanical qualities. Following the recommendations of the American Society for Testing and Materials (ASTM) A370 and ASTM A675, the testing was done on five steel bars for each bar size.

2.3 Loading rate:

The rate at which the load is applied during the testing procedure is referred to as the load rate, and it is used to calculate a squat wall's in-plane shear capacity. The rate at which the applied load rises in relation to time or displacement is known as the load rate.

The testing apparatus or equipment utilised is often what regulates the load rate in experimental testing. Up until the required load level is attained or a failure occurs, the load is gradually

increased. To guarantee precise readings and to record the behaviour of the wall under increasing weights, the load rate is carefully regulated.

A squat wall's in-plane shear capacity is assessed during testing by keeping an eye on the load-displacement response. The in-plane shear capacity of the wall may be thought of as the greatest load that can be applied before failure or severe deformation. Faster load rates may result in different failure modes or behaviours compared to slower load rates, which might have an impact on the observed behaviour and final capacity of the wall.

Depending on the particular testing standards or specifications being followed, the loading rate ranges might change. However, the following are rough ranges for several kinds of loading rates:

1. Quasi-Static Loading: Usually between 0.1 and 10 mm/min, or millimetres per minute or slower.

2. Slow loading: Usually between one and one hundred centimetres per minute.

3. Medium Loading: Usually between 10 and 100 decimeters per minute (dm/min).

4. Rapid loading: Usually occurring at speeds of one to ten metres per minute or even more quickly.

The specimens were loaded slowly during the experiment, at a pace of 1 mm/sec. It was noted, nonetheless, that maintaining this precise loading rate during the test was difficult.

Chapter-3

3 TEST RESULTS:

Under the same testing conditions, the specimens were subjected to load applied in the form of displacement using a hydraulic jack. The results of the testing revealed that Specimen Wall 1:2 exhibited the highest maximum load capacity among the three specimens, withstanding a load of 168 kN at a displacement of 10.42 mm. On the other hand, Wall 2:1 displayed the lowest maximum load capacity, with a load of 130 kN at a displacement of 8.2 mm.

During the testing process, it was observed in all three specimens that the loading rate decreased once cracks started to appear at the corners of the openings. This behavior is consistent with the anticipated response of shear walls with openings. Additionally, the initial cracking in all specimens was observed to initiate from the corners of the openings.

As the testing progressed, failure occurred at the bottom of the specimens when the compression web of the wall crushed, and tensile cracks were observed in the bottom tensile portion of the wall. The experiment was terminated when the load started to decrease significantly with a noticeable displacement, indicating a significant reduction in the load-carrying capacity of the specimens.

Overall, the comparative testing of the specimens under the same conditions provided realistic insights into their performance, including load capacity, crack initiation, and failure modes. These observations contribute to a better understanding of the behavior of shear walls with different aspect ratios of openings.

3.1 Wall 1:2:

The tested wall demonstrated a maximum peak load capacity of 168 kN. Initially, the relationship between load and displacement was directly proportional, indicating a linear behavior. However, as the testing progressed, cracks began to appear at the top corner of the opening, resulting in a decrease in the rate of force application.

As the cracks propagated and reached the top beam and foundation, the slope of the load versus displacement curve became milder. This behavior can be attributed to the redistribution of forces within the wall and the interaction between the cracks and the surrounding structural elements.

Eventually, the load started to decline, and the cracks widened, indicating a loss of load-carrying capacity and structural integrity. At this point, the experiment was terminated to prevent further damage and potential failure.

The observations during the testing process provide valuable information about the structural behavior of the wall, specifically in terms of crack initiation, crack propagation, and the ultimate failure mechanism.

Figure 9 : Wall 1:2 Experimental Setup

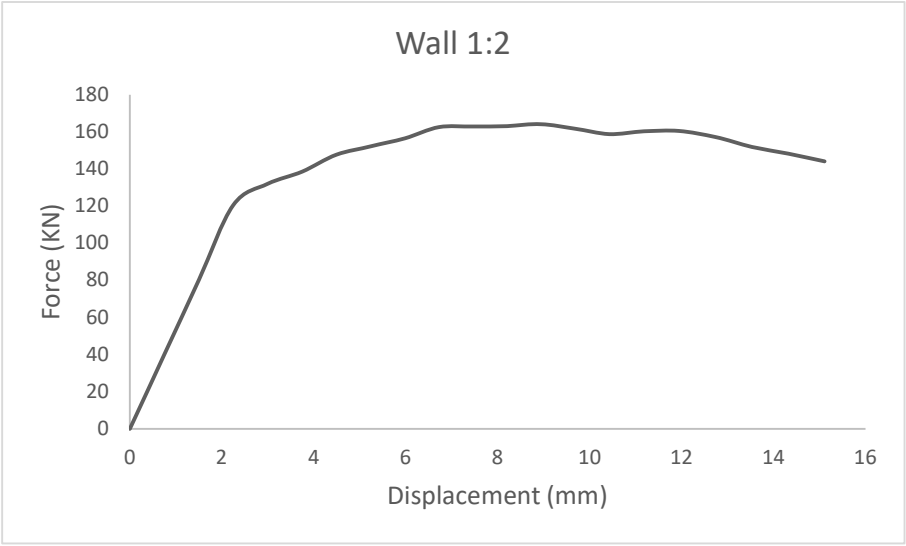

Figure 10: Wall 1:1 Experimental Load Vs Displacement Graph

3.2 Wall 1:1:

The wall with an aspect ratio of 1:1 exhibited a maximum peak load of 150 kN in terms of its in-plane shear capacity. During the loading process, cracks started to appear in the wall, indicating the initiation of localized damage. These cracks were observed to be scattered across the wall surface rather than concentrated in specific areas.

As the load continued to increase, the concrete within the wall began to undergo compression failure. This failure occurred when the compressive stress exceeded the capacity of the concrete to withstand it. At this point, the load-bearing capacity of the wall started to decrease significantly.

The occurrence of compression failure in the concrete resulted in a reduction in the load-carrying capacity of the wall. As the cracks widened and propagated, the ability of the wall to resist shear forces decreased. This led to a substantial decline in the applied load as the structural integrity of the wall was compromised.

Overall, the wall with an aspect ratio of 1:1 demonstrated a lower in-plane shear capacity compared to other specimens. The scattered pattern of cracks and the subsequent compression failure of the concrete played a significant role in determining the maximum load that the wall could withstand.

Figure 11 : Wall 1:1 Crack Pattern

Figure 12 : Wall 1:1 Experimental Load Vs Displacement Graph

3.3 Wall 2:1:

Among the three walls with different aspect ratios, the wall with an aspect ratio of 1:2 exhibited the worst performance in terms of in-plane shear capacity. It reached a maximum peak load of 130 kN, which was the lowest among the three specimens. The behavior of this wall during the test can be described in several stages.

Initially, as the load was applied, the wall demonstrated a linear relationship between the applied load and displacement. However, as the load increased, cracks started to appear at the corner of the opening. These cracks indicated the initiation of localized damage within the wall.

As the displacement increased further, the cracks continued to propagate, reaching the top beam of the wall at a displacement value of 7.2 mm. This indicated that the damage was spreading throughout the wall, affecting its overall structural integrity.

At a displacement value of 8.2 mm, the load started to decrease significantly. This decline in the load-bearing capacity can be attributed to the formation and widening of cracks, leading to the loss of shear resistance in the wall.

The occurrence of cracks at the corners of the opening is likely due to stress concentration in these areas. The presence of an opening disrupts the continuity of the wall, causing stress concentrations at the corners. This ultimately leads to the initiation and propagation of cracks in these vulnerable regions.

The decrease in load after reaching the peak value can be attributed to the compression failure of the concrete within the wall. As the load increased, the compressive stress exceeded the capacity of the concrete, resulting in its failure under compression. This failure reduced the load-carrying capacity of the wall significantly.

The poor performance of the wall with a 1:2 aspect ratio can be attributed to several factors. The elongated shape of the opening in this wall creates more stress concentration points,

making it more susceptible to failure. Additionally, the aspect ratio affects the distribution of forces within the wall, leading to an imbalance in load-bearing capacity.

The limited in-plane shear capacity of this wall highlights the importance of proper design and reinforcement detailing, especially when openings are incorporated. The presence of openings, even for architectural purposes, can significantly compromise the structural performance of shear walls.

Overall, the behavior of the wall with a 1:2 aspect ratio indicates the need for careful consideration and design optimization when incorporating openings in shear walls. The detrimental effects of openings on the load-carrying capacity and the formation of cracks emphasize the importance of reinforcement detailing and strengthening measures to enhance the structural performance of such walls.

Figure 13: Wall 2:1 Experimental Setup

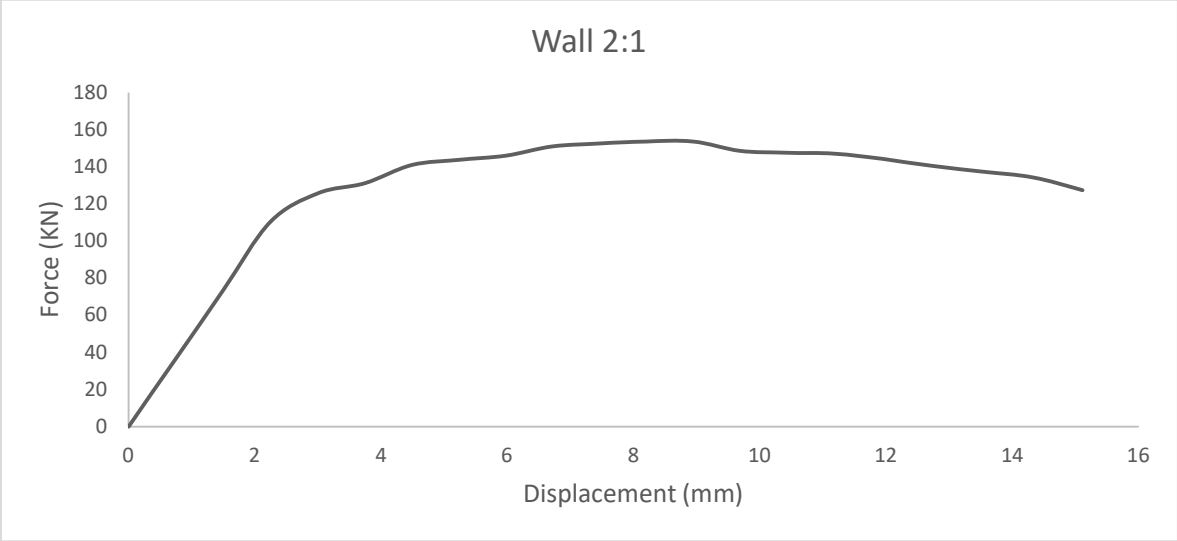

Figure 14: Wall 2:1 Experimental Load Vs Displacement Graph

3.4 Comparison:

Among the three walls with different aspect ratios, the wall with an aspect ratio of 1:2 exhibited the highest in-plane shear capacity, reaching a peak load of 164.25 kN at a displacement of 9 mm. This wall outperformed the other two specimens in terms of its load-carrying capacity. The behavior of this wall during the test can be analyzed in multiple stages.

During the initial loading phase, the wall demonstrated a proportional relationship between the applied load and displacement. As the load increased, the wall exhibited good resistance to shear forces, leading to a gradual increase in the applied load.

At a displacement of 9 mm, the wall reached its peak load capacity of 164.25 kN. This indicates that the wall was able to withstand significant shear forces before reaching its maximum load-carrying capacity. The high shear capacity of this wall can be attributed to its aspect ratio, which provided a favorable distribution of forces within the wall.

In terms of failure modes, the wall with a 1:2 aspect ratio experienced a combined flexural-shear failure. This suggests that the wall exhibited a combination of flexural bending and shear deformation before reaching its ultimate failure point. This behavior indicates that the wall had a higher resistance to both bending and shear forces.

On the other hand, the wall with a 2:1 aspect ratio exhibited the lowest shear capacity among the three specimens. It reached a peak load of 130.47 kN at a displacement of 7 mm, indicating a lower load-carrying capacity compared to the other walls. The failure mode observed in this wall was predominantly shear failure, indicating that it had a lower resistance to shear forces.

The wall with a 1:1 aspect ratio showed an intermediate in-plane shear capacity. It reached a peak load of 153.71 kN at a displacement of 8 mm. The failure mode observed in this wall involved concrete crushing at the compression web bottom, suggesting that the failure mechanism was influenced by both shear and compression forces.

The results from Table 2 indicate the relative performance of each wall in terms of their load-displacement behavior. The ratio of shear capacities provides a quantitative comparison between the walls, with the 1:2 aspect ratio wall exhibiting the highest ratio of 1.26, followed by the 1:1 aspect ratio wall with a ratio of 1.18, and the 2:1 aspect ratio wall with a ratio of 1.00.

The superior performance of the wall with a 1:2 aspect ratio can be attributed to its geometry, which provides a balanced distribution of forces and a higher resistance to both flexural and shear deformation. The lower shear capacity of the 2:1 aspect ratio wall suggests that the elongated shape of the opening in this configuration might have compromised the overall strength and integrity of the wall.

These findings highlight the importance of aspect ratio and reinforcement detailing in the design of shear walls. Proper consideration of these factors can significantly influence the load-carrying capacity and failure modes of squat walls with openings.

In summary, the wall with a 1:2 aspect ratio exhibited the highest in-plane shear capacity, while the wall with a 2:1 aspect ratio demonstrated the lowest shear capacity. The failure modes varied, with the 1:2 aspect ratio wall experiencing combined flexural-shear failure, the 1:1 aspect ratio wall showing concrete crushing at the compression web bottom, and the 2:1 aspect ratio wall exhibiting pure shear failure. These findings emphasize the significance of aspect ratio and reinforcement design in optimizing the performance of squat walls with openings.

Table 2: Displacement At Peak loads

Specimen	Displacement (mm)	Load (KN)	Ratio
Wall 1:2	9	164.25	1.26
Wall 1:1	8	153.71	1.18
Wall 2:1	7	130.47	1.00

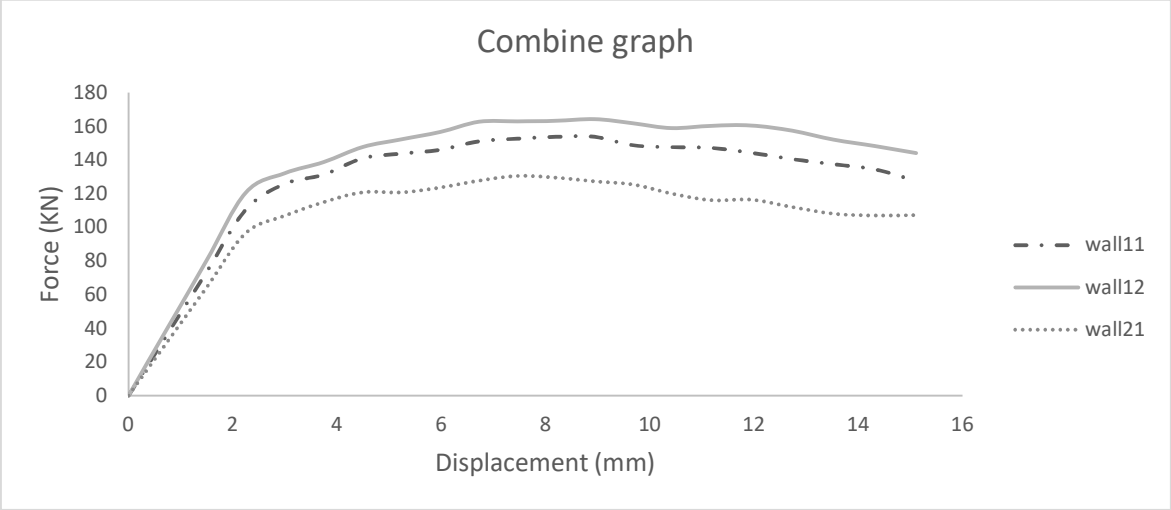

Figure 15: Combined Experimental Load Displacement Graph

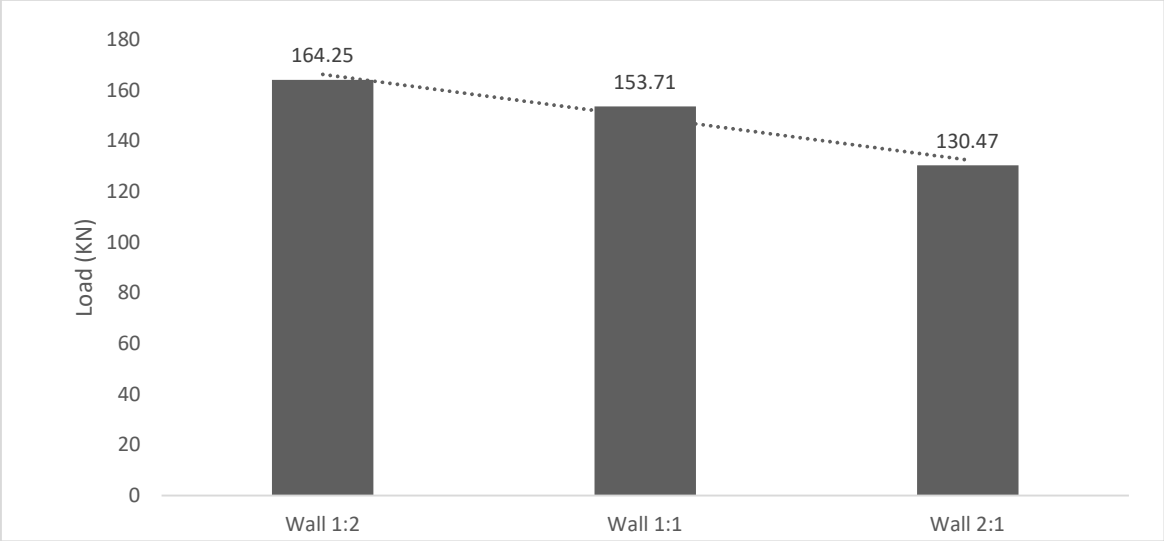

Figure 16: Experiemntal Peak Loads

Chapter-4

4 Numerical model:

In this study, the finite element analysis package Abaqus 2020 was chosen as the software for modeling and analyzing the three specimens. Abaqus is widely recognized for its robustness, accuracy, fidelity, and computational power, making it a suitable choice for conducting this research.

Using Abaqus, the three specimens with different aspect ratios were carefully modeled to simulate their real-life behavior. The software allows for the creation of detailed and accurate finite element models, capturing the geometric complexity and material properties of the specimens.

To ensure the reliability of the numerical analysis, the models were validated by comparing their results with the experimental data obtained from the physical testing of the specimens. This validation process is crucial in verifying the accuracy and predictive capabilities of the finite element models.

By analyzing the models in Abaqus, various parameters and response variables, such as displacements, stresses, and strains, were obtained. These results were then compared to the experimental data to assess the accuracy and effectiveness of the numerical analysis.

Abaqus provides advanced analysis capabilities, including the ability to incorporate material models, load conditions, and boundary conditions that accurately represent the behavior of the real-world structures. This allows for a comprehensive analysis of the squat walls with openings, considering factors such as nonlinearity, material damage, and complex loading conditions.

Overall, the selection of Abaqus 2020 as the finite element analysis package for this study ensures the reliability and accuracy of the numerical analysis. It allows for the simulation of the behavior of the specimens, providing valuable insights into their structural performance, failure mechanisms, and load-carrying capacities.

4.1 General description

To validate the load-displacement relationship, a finite element model was developed in ABAQUS software version 2020. This section provides an overview of the modeling approach and the software used.

2. Component Modeling:

The model consisted of three main components: the beam, web, and foundation. Each component was separately modeled using parts in the 3D modeling space and defined as deformable type. The base feature was created as a solid shape using the extrusion type.

3. Merging Components:

After modeling the individual components, they were merged together to create a single part representing the complete squat wall specimen. This step ensured the integration of all components for accurate simulation.

4. Reinforcement Modeling:

The reinforcement was modeled using wire shapes and defined as planner type. This allowed for the representation of steel reinforcement in the model and consideration of its interaction with the concrete.

5. Concrete Modeling:

For the concrete material, a 3-Dimensional 8-noded brick element (C3D8R) was employed. This element is suitable for modeling the behavior of concrete in three dimensions, capturing its nonlinear response under load.

The 3-Dimensional 8-noded brick element (C3D8R) is a type of finite element used in structural analysis and numerical simulations. It is designed to represent solid three-dimensional objects, such as concrete structures, accurately and efficiently.

The term "8-noded" refers to the number of nodes or vertices that define the shape of the element. In the case of the C3D8R element, there are eight nodes, allowing for a higher level of accuracy in representing complex geometries and capturing the behavior of the structure under different loading conditions.

The C3D8R element is commonly used in finite element analysis software, such as ABAQUS, for simulating the behavior of solid materials like concrete. It can accurately capture the response of the material to various mechanical loads, including compression, tension, and shear.

By discretizing the three-dimensional domain into smaller elements, such as the C3D8R, the software can analyze the deformation, stresses, and strains within the material. This enables engineers and researchers to study the structural behavior, predict failure mechanisms, and optimize designs for improved performance and safety.

The C3D8R element incorporates various mathematical formulations and numerical algorithms to accurately represent the nonlinear behavior of materials, such as concrete. These formulations take into account factors like material properties, boundary conditions, and loading conditions to provide realistic and reliable results.

In summary, the 3-Dimensional 8-noded brick element (C3D8R) is a versatile and widely used finite element in structural analysis. It allows for accurate representation of solid three-dimensional objects and is especially useful for simulating the behavior of materials like concrete under different loading conditions. Its application in software packages like ABAQUS provides engineers and researchers with valuable insights into the performance and response of structures, aiding in the design and analysis processes.

6. Sensitivity Analysis:

A sensitivity analysis was conducted to determine the optimum mesh size for the model. By varying the mesh size and evaluating the resulting response, a mesh size of 50mm was identified as providing reliable results with an appropriate balance between accuracy and computational efficiency.

In Abaqus, mesh size refers to the discretization of a geometric domain into smaller elements. The choice of mesh size is an important consideration in finite element analysis as it can impact the accuracy and computational efficiency of the simulation.

The mesh size in Abaqus is determined by the element size, which defines the dimensions of the individual elements used to approximate the geometry. The element size can be specified based on factors such as the desired level of accuracy, complexity of the model, and computational resources available.

Sensitivity analysis is a technique used to determine the effect of changing certain parameters on the results of a simulation. In the context of mesh size in Abaqus, a sensitivity analysis can be performed to evaluate the influence of different mesh sizes on the accuracy and convergence of the analysis.

To conduct a sensitivity analysis for mesh size, the finite element model is analyzed using different element sizes, typically ranging from coarse to fine. The analysis results, such as displacements, stresses, or strains, are compared across the different mesh sizes to assess the sensitivity of the results to changes in mesh size.

The sensitivity analysis helps in determining an appropriate mesh size that strikes a balance between accuracy and computational efficiency. A mesh that is too coarse may result in inaccurate results, while a mesh that is too fine can significantly increase the computational time and resources required. By evaluating the convergence of the analysis results with different mesh sizes, engineers and researchers can select an optimum mesh size that provides reliable and efficient results for their specific analysis. It is important to note that the sensitivity analysis for mesh size is specific to the particular problem being analyzed and the desired level of accuracy. Different types of simulations and materials may require different mesh sizes, and it is generally recommended to conduct sensitivity analyses to validate the chosen mesh size for a specific analysis.

7. Interface Modeling:

To simulate the interface between the concrete and steel embedded regions, a constraint was applied. This specification ensured the realistic modeling of the bond between these two materials and their interaction under load.

The properties of the embedded region in the context of finite element analysis refer to the characteristics and behavior of the material or component that is embedded within the larger structure being analyzed. The embedded region is typically modeled as a separate entity within the finite element model, and its properties are defined based on its specific material composition and behavior.

The properties of the embedded region can vary depending on the nature of the material being modeled. For example, if the embedded region represents a reinforcing steel bar embedded

within concrete, the properties may include the elastic modulus, yield strength, and Poisson's ratio of the steel material.

In addition to the mechanical properties, other properties such as the geometry, orientation, and location of the embedded region can also be defined. These properties play a significant role in accurately representing the behavior of the embedded region within the overall structural analysis.

In some cases, additional parameters or constraints may need to be specified to ensure the appropriate interaction between the embedded region and the surrounding materials. This may involve defining contact properties, such as friction or adherence, between the embedded region and the adjacent elements.

It is essential to accurately define the properties of the embedded region to ensure the reliability and accuracy of the finite element analysis. The properties are typically derived from experimental data or from established material models and guidelines specific to the material or component being modeled.

By properly defining the embedded region properties, engineers and researchers can simulate the behavior of the embedded component and evaluate its impact on the overall structural performance. This allows for a more comprehensive and accurate analysis of the complete system.

8. Boundary Conditions:

The boundary conditions of the physical testing setup were replicated in the model. The bottom surfaces of all three walls were restrained from displacement and movement, accurately simulating the fixed boundary conditions.

By applying the encastra boundary condition, you can simulate a fully fixed or clamped connection in your structural analysis, which can be useful in studying the behavior of structures under fixed supports or in evaluating the effects of rigid connections on the overall system response.

9. Loading Conditions:

The load was applied on the top beam in the X-direction, replicating the experimental setup where the load was applied as displacement. This loading condition allowed for the evaluation

of the load-displacement relationship and determination of the in-plane shear capacity

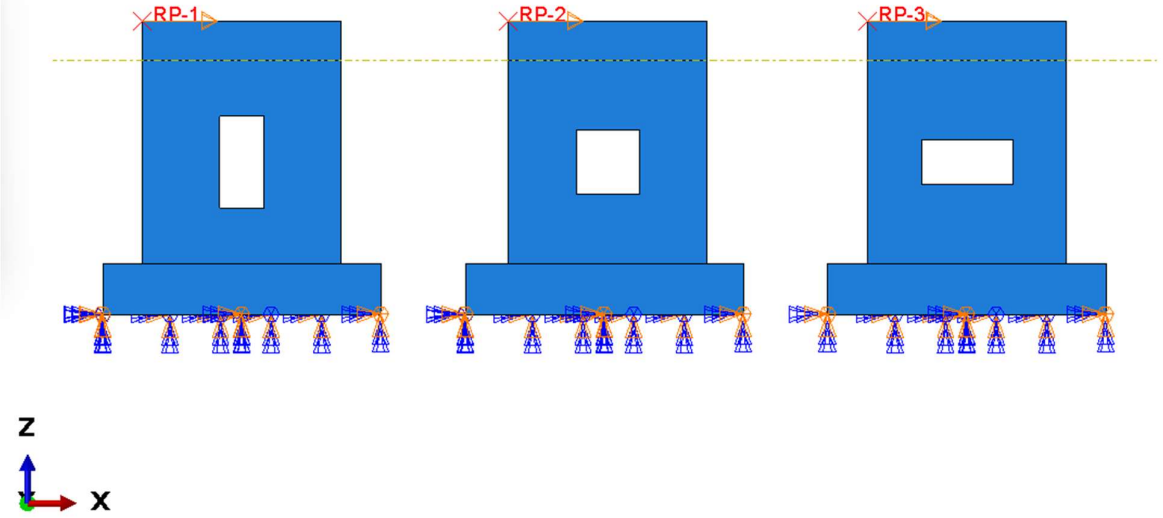

Figure 17: Load Direction

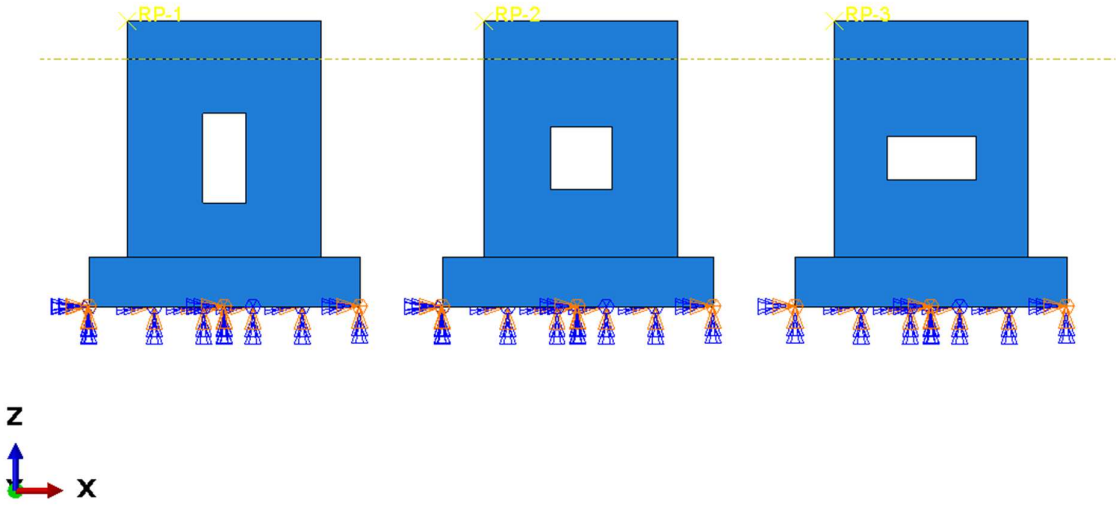

Figure 18: Boundary Condition

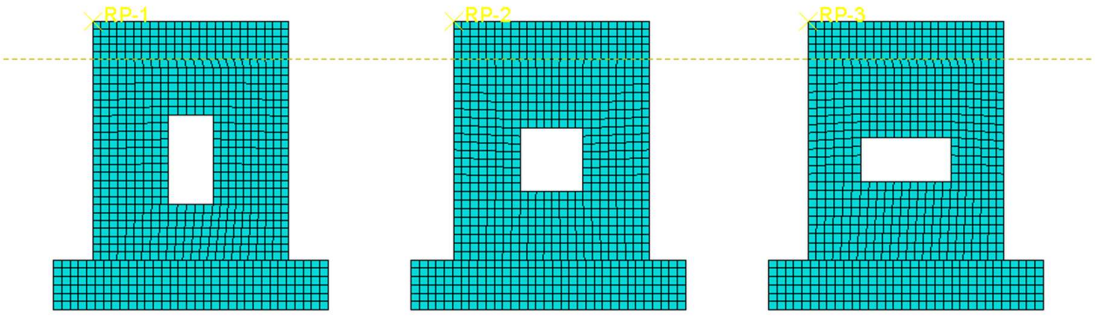

Figure 19: Model Mesh

4.2 Material behavior

The Concrete Damage Plasticity (CDP) model is a widely used approach in simulating the behavior of concrete. It is a plasticity-based continuum damage model that takes into account the two primary failure mechanisms: compression damage and tension damage. These mechanisms play a crucial role in the structural response of concrete elements under various loading conditions. By incorporating these failure mechanisms, the CDP model provides a comprehensive understanding of concrete behavior.

To quantify the extent of compression and tension damage, the CDP model utilizes two damage variables: dc for compression damage and dt for tension damage. These variables are unitless and range from 0 to 1. A value of 1 indicates complete failure, while a value of 0 represents intact material. As the plastic deformation in the concrete increases, these damage variables also increase, reflecting the progression of damage within the material.

The development of the damage parameters in the CDP model is based on elasticity theory. Specifically, the equivalent compressive plastic strain (ε_c^pl) and the equivalent tensile plastic strain (ε_t^pl) govern the evolution of the yield strain, which is associated with failure mechanisms under compression and tension loads. These strains capture the inelastic behavior of the concrete and determine the damage progression.

By considering the relationship between stress and strain, the CDP model can accurately predict the response of concrete under uniaxial compression and tension loads. The stress-strain relationships for these loading conditions are determined based on the CDP model's formulation and can be expressed through mathematical equations. These relationships provide insights into the material's behavior, including the onset of damage, the peak stress, and the post-peak softening behavior.

Overall, the CDP model is a valuable tool in simulating the behavior of concrete, as it captures the key failure mechanisms and provides a realistic representation of the material's response. By incorporating the damage variables, the model can accurately predict the progression of damage and assess the structural integrity of concrete elements under different loading

scenarios. This enables engineers to analyze and design concrete structures with enhanced accuracy and reliability.

$$\sigma_t = (1 - d_t)E_o(\varepsilon_t - \varepsilon_t{}^{pl}) \quad \text{(xx)}$$

$$\sigma_c = (1 - d_c)E_o(\varepsilon_c - \varepsilon_c{}^{pl}) \quad \text{(xx)}$$

In the CDP model, the initial modulus of elasticity (E_o) represents the stiffness of the material in its undamaged state. This parameter is an important input for capturing the elastic behavior of the material. It reflects the material's ability to resist deformation and provides a measure of its initial stiffness. The total strain (ε_t) experienced by the material is a key variable in the CDP model. It represents the overall deformation of the material under applied loads. By tracking the total strain, the model can monitor the extent of deformation and assess the material's response to external forces.

To consider the biaxial behavior of the material, the ratio of equi-biaxial compressive yield stress to uniaxial compressive yield stress is taken into account. This ratio provides a measure of the material's strength under different stress states. By considering the biaxial behavior, the CDP model can more accurately simulate the material's response to complex loading conditions and capture the interaction between different stress components. In addition to these parameters, the CDP model incorporates various flow parameters to simulate the plastic flow of the material. These parameters, including the flow potential eccentricity, viscosity, dilation angle, and bulk modulus, provide insights into the material's plastic behavior, such as the rate of plastic deformation, volume change, and energy dissipation. By incorporating these flow parameters, the CDP model can capture the complex plastic behavior and accurately predict the material's response under different loading scenarios.

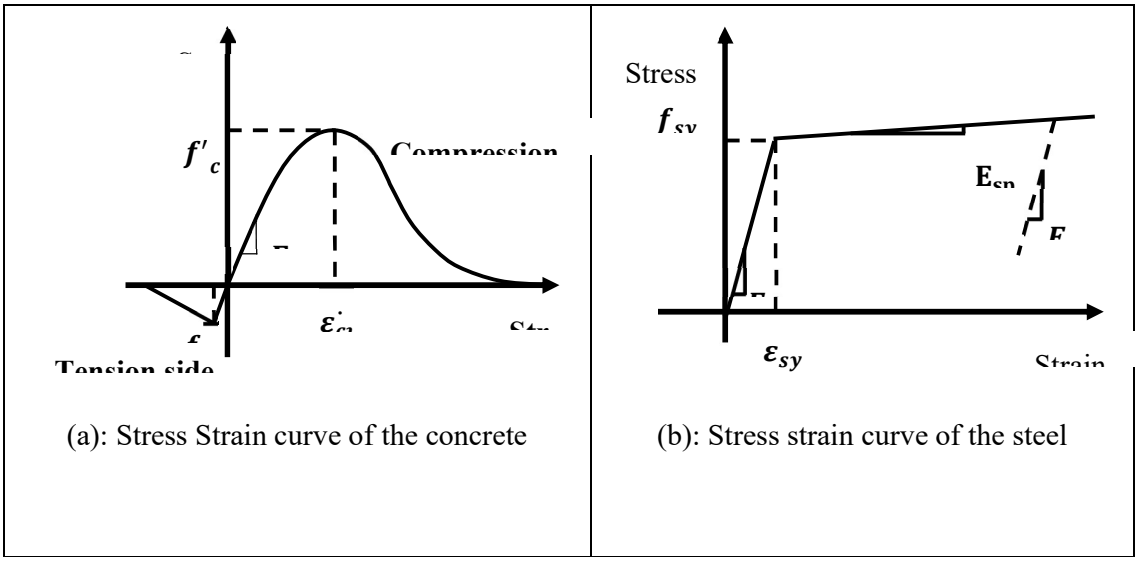

(a): Stress Strain curve of the concrete

(b): Stress strain curve of the steel

Figure 20: Material Models

The compressive strength (fc') of the concrete is given as 24 MPa, indicating the maximum compressive stress that the material can withstand. The Poisson's ratio, which represents the lateral contraction of the material when subjected to axial loading, is provided as 0.19. The density of the concrete is given as 2.4 g/cm3, indicating its mass per unit volume.

Table 5 provides properties and variables for the yield tensile strength. The yield tensile strength represents the maximum tensile stress that the material can sustain before experiencing plastic deformation. In this case, the yield tensile strength is specified as 345 MPa. The Poisson's ratio for the material is given as 0.3, indicating the ratio of lateral contraction to axial extension under tensile loading. The density of the material is provided as 8.05 g/cm3, indicating its mass per unit volume.

These material parameters play a crucial role in the concrete damage plasticity (CDP) model. They determine the material's response to various loading conditions, including compression, tension, and shear. The values of these parameters influence the behavior of the material, such as its stiffness, strength, and deformation characteristics.

By specifying the appropriate material parameters in the CDP model, it is possible to accurately simulate and predict the behavior of the concrete under different loading scenarios. These parameters allow for the accurate representation of the material's response to stress and strain, enabling engineers to assess the structural performance and integrity of concrete components and structures.

4.2.1 Steel constitutive model

The CEB code [76] recommended model Validation of the ABAQUS model. For modeling reinforcement steel elastic-plastic constitutive model with strain hardening has been deployed. Elastic modulus, yielding stress, yielding strains and post yielding modulus are represented by E_s, f_{sy}, ε_{sy} and E_{sp} respectively. This section compares experimental result with ABAQUS results. Additionally, Abaqus crack pattern has also been presented. And it was found that they are in close match with experimental results.

Chapter-5

5 Numerical Results:

After performing a detailed modeling and analysis using the developed finite element model, the load versus displacement graph was obtained. The reaction force in the x-direction was determined by summing the reaction forces of all the bottom nodes in the model. Displacements were measured at the top node of the beam, corresponding to the experimental setup.

From the analysis results, several key findings were extracted. These findings provide insights into the behavior and performance of the modeled system. The load versus displacement graph illustrates the relationship between the applied load and the resulting displacement, providing a quantitative representation of the system's response to loading.

By examining the load versus displacement graph, engineers and researchers can assess the structural integrity and load-carrying capacity of the system. This information is crucial for evaluating the performance and safety of the structure under different loading conditions. Additionally, the obtained reaction forces and displacements serve as important indicators of the system's response to external forces, providing valuable data for further analysis and design considerations.

5.1 Wall 1:2:

During the analysis, it was observed that the wall exhibited linear elastic behavior up to a displacement of 1.5mm, while carrying an in-plane shear load of 110KN. However, as the load increased, cracks began to appear, and the load-displacement graph transitioned into a milder slope. This change in behavior indicated the onset of plastic deformation in the embedded vertical steel.

As the load continued to increase, the wall reached its maximum load capacity of 168.64KN at a displacement of 11.4mm. At this point, the cracks in the wall had widened, and the load-displacement graph showed a decreasing trend. This decline in load indicated that the wall had undergone significant deformation and was no longer able to sustain the applied load.

The milder portion of the load-displacement graph, which corresponded to the plastic deformation of the embedded vertical steel, indicated the redistribution of forces within the wall. This plastic deformation allowed the structure to absorb energy and redistribute the load, which contributed to the wall's ability to sustain higher loads before reaching its ultimate failure point.

Overall, the observed behavior of the wall demonstrated a combination of elastic and plastic deformation, with the embedded vertical steel playing a crucial role in dissipating energy and providing ductility to the structure. Understanding these behaviors is important for designing resilient structures that can withstand varying load conditions and mitigate the risk of failure.

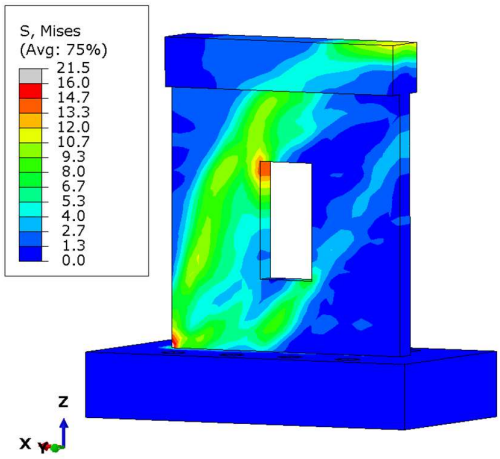

Figure 21: Von Mises stress

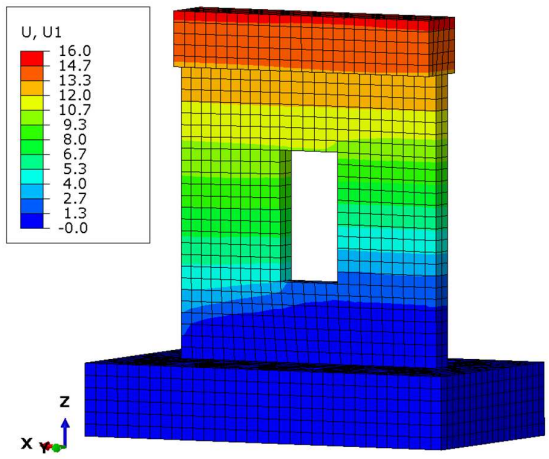

Figure 22: Displacement U1,

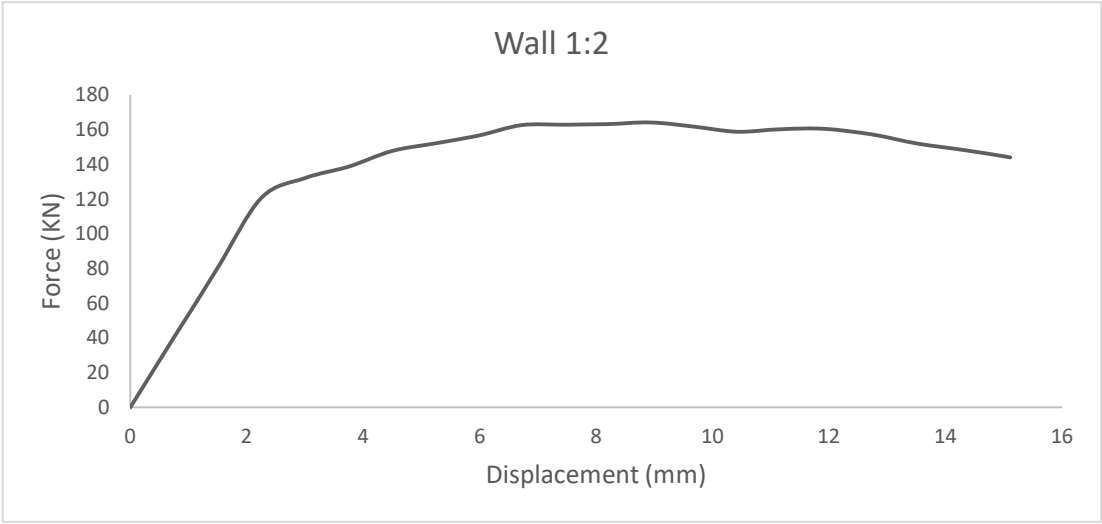

Figure 23: Wall 1:2 Numerical Load Vs Displacement Graph

5.2 Wall 2:1

Wall 2:1, with its smaller shear area, exhibited the lowest in-plane shear capacity among the three walls, reaching a maximum load of 130.6 KN at a displacement of 8.2mm. This lower shear capacity can be attributed to the reduced cross-sectional area available for resisting shear forces, resulting in a lower load-carrying capacity compared to the other walls.

The failure mode observed in Wall 2:1 was pure shear, as indicated by the deformed shape of the wall. Pure shear failure occurs when the material experiences shear stresses that exceed its shear strength, leading to localized shear cracks and failure. In this case, the reduced shear area of Wall 2:1 resulted in a lower capacity to resist shear forces, leading to the observed pure shear failure.

Additionally, it was observed that the compression web of Wall 2:1 experienced higher stresses compared to the tension web. This is expected as the compression web carries the compressive loads, while the tension web primarily carries tensile loads. The higher stresses in the compression web can be attributed to the distribution of shear forces and the resulting load transfer mechanisms within the wall. Understanding the failure mode and stress distribution in Wall 2:1 is essential for evaluating its structural performance and determining its suitability for specific design requirements. The findings highlight the importance of considering the shear area and load distribution in the design of squat walls to ensure their ability to resist shear forces and prevent shear failure.

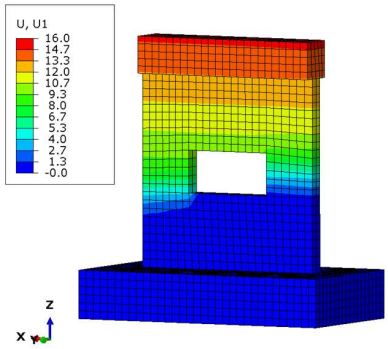

Figure 24: Displacement U1,

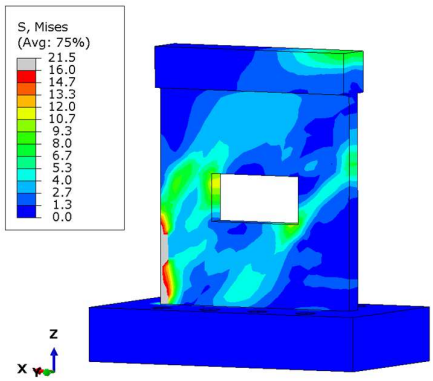

Figure 25: Von Mises stress

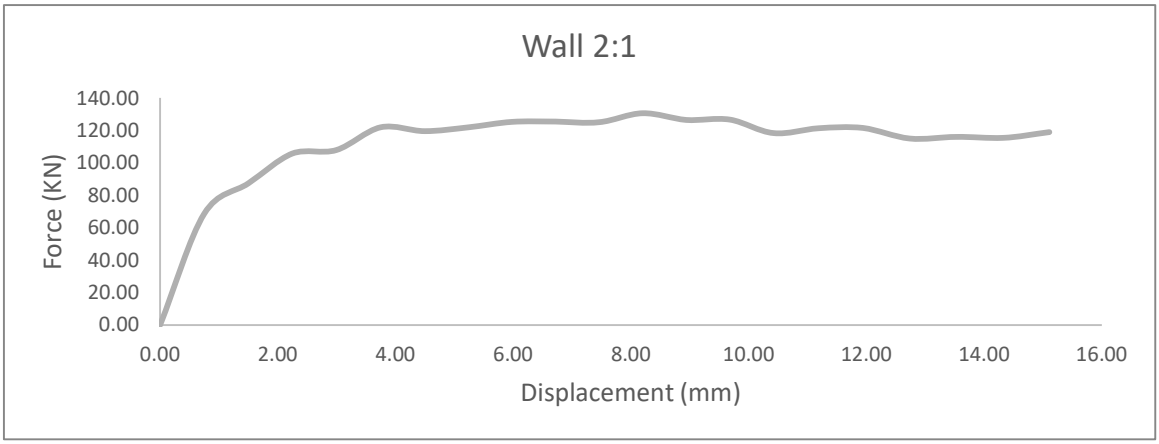

Figure 26: Wall 2:1 Numerical Load Vs Displacement Graph

5.3 Wall 1:1

Wall 1:1 exhibited a behavior that falls between the other two walls in terms of its shear capacity. It displayed high compressive stresses at the bottom compression web, indicating its ability to resist compression forces effectively. The analysis results revealed that this wall could

sustain a peak load of 155.4 KN at a displacement value of 10.4mm, which indicates a relatively higher load-carrying capacity compared to Wall 2:1 but lower than Wall 1:2.

The load vs displacement graph obtained from the analysis provides valuable insights into the wall's behavior. Initially, the graph shows a linear relationship between load and displacement, indicating an elastic response of the wall. However, as the load increased, cracks started to appear, and the graph displayed a milder slope. This change in slope indicates the onset of plastic deformation and the development of cracks within the wall.

The obtained load vs displacement graph demonstrates the wall's ability to sustain increasing loads up to its peak capacity. The peak load of 155.4 KN corresponds to a displacement value of 10.4mm, beyond which the load started to decline significantly. This indicates that the wall reached its ultimate capacity and experienced structural failure.

The behavior of Wall 1:1, with its intermediate shear capacity and high compressive stresses at the bottom compression web, suggests that it could be suitable for certain structural applications where a balance between shear resistance and load-carrying capacity is desired. However, further analysis and evaluation are necessary to fully understand the wall's performance and its suitability for specific design requirements.

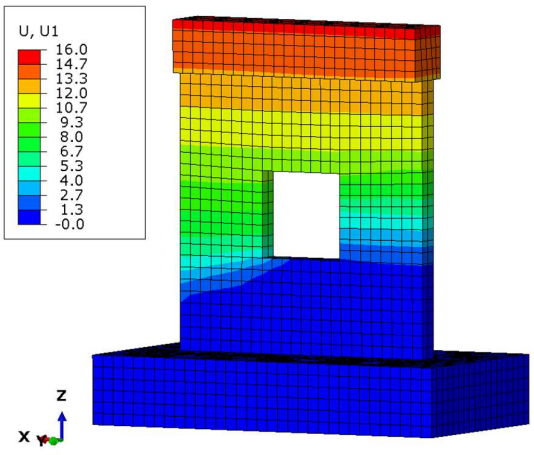

Figure 27: Displacement U1,

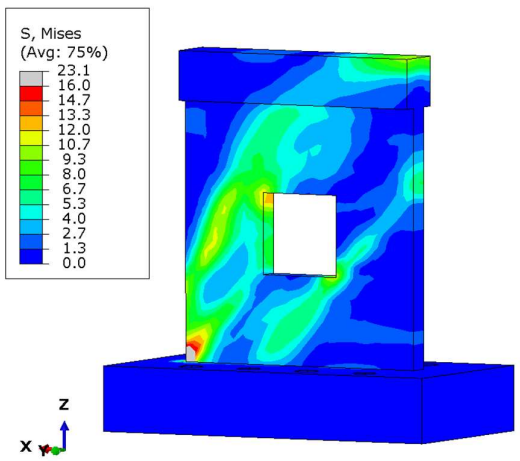

Figure 28: Von Mises stress

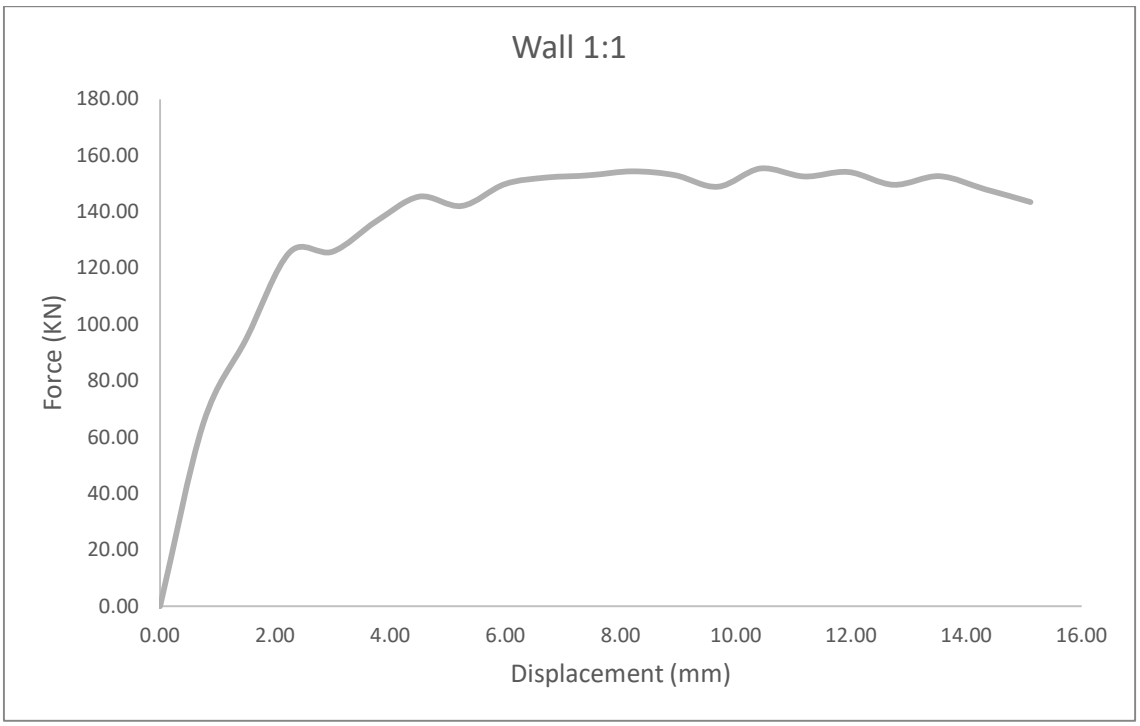

Figure 29: Wall 1:1 Numerical Load Vs Displacement Graph

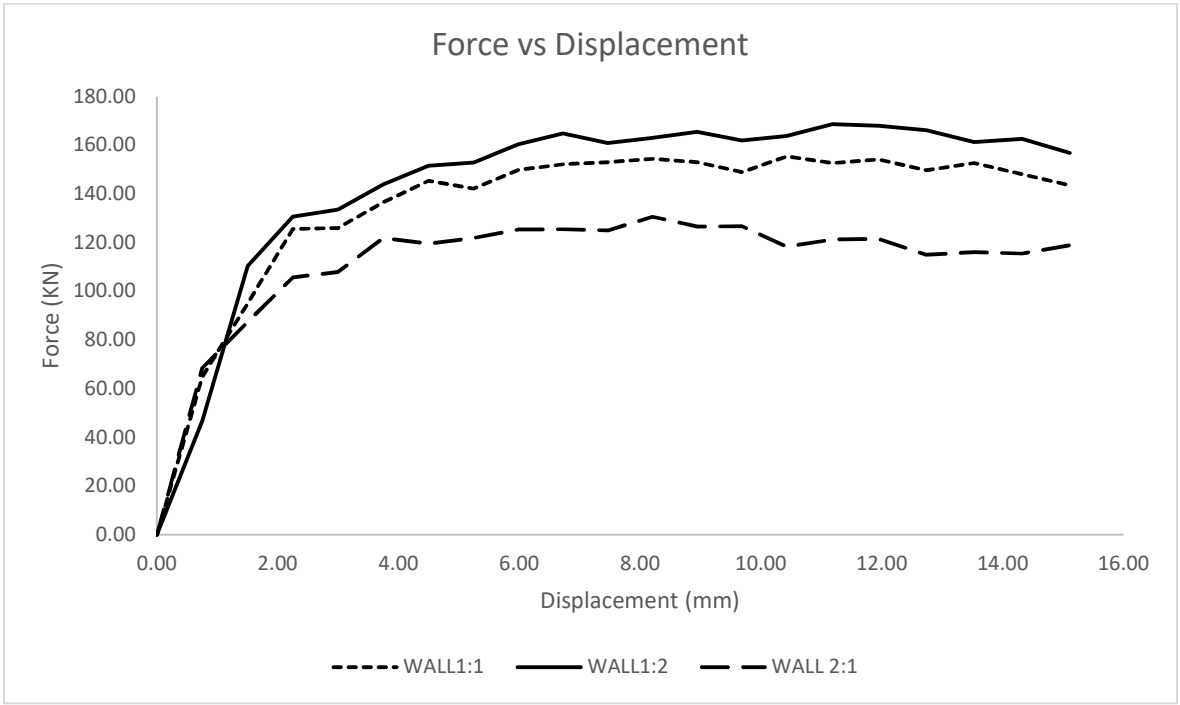

Figure 30: Combined Numerical Load Displacement Graph

Chapter-6

6 Comparison:

A comprehensive comparison between the numerical and experimental analyses was conducted for all the mentioned specimens. The results revealed a remarkable similarity between the numerical predictions and the experimental measurements. This close match between the two sets of data indicates the accuracy and reliability of the numerical analysis in capturing the behavior of the specimens.

The comparison was performed by plotting the load vs displacement graphs obtained from both the numerical and experimental analyses. Upon visual inspection, it was evident that the two sets of data exhibited a high degree of similarity, with the numerical results closely following the experimental trends. This agreement between the numerical and experimental results further validates the effectiveness of the numerical modeling approach in simulating the real-world behavior of the specimens.

The close match between the numerical and experimental analyses provides confidence in the accuracy of the numerical model and its ability to capture the essential features and response of the specimens. This agreement also highlights the success of the chosen modeling techniques, material properties, and boundary conditions used in the numerical simulations.

It is important to note that while the numerical results closely align with the experimental data, there may still be minor discrepancies due to inherent uncertainties and variations between the real-world behavior and the numerical representation. Nevertheless, the overall agreement between the two sets of results strengthens the confidence in the numerical analysis and its applicability for studying the behavior of similar structural systems in future studies.

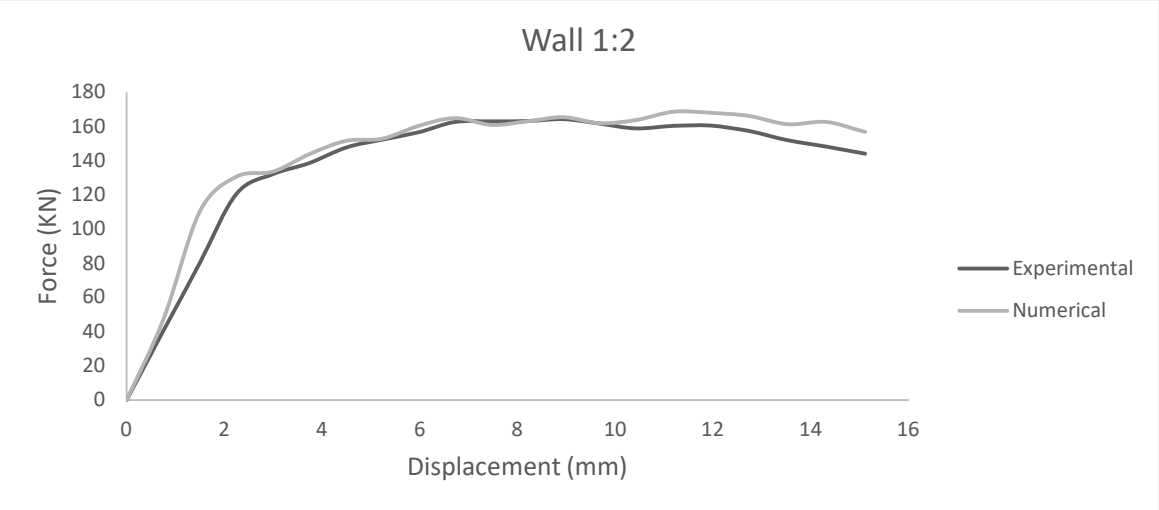

Figure 31: Wall 1:2 Experimental Vs Numerical Load Displacement Graph

Figure 32: Wall 1:1 Experimental Vs Numerical Load Displacement Graph

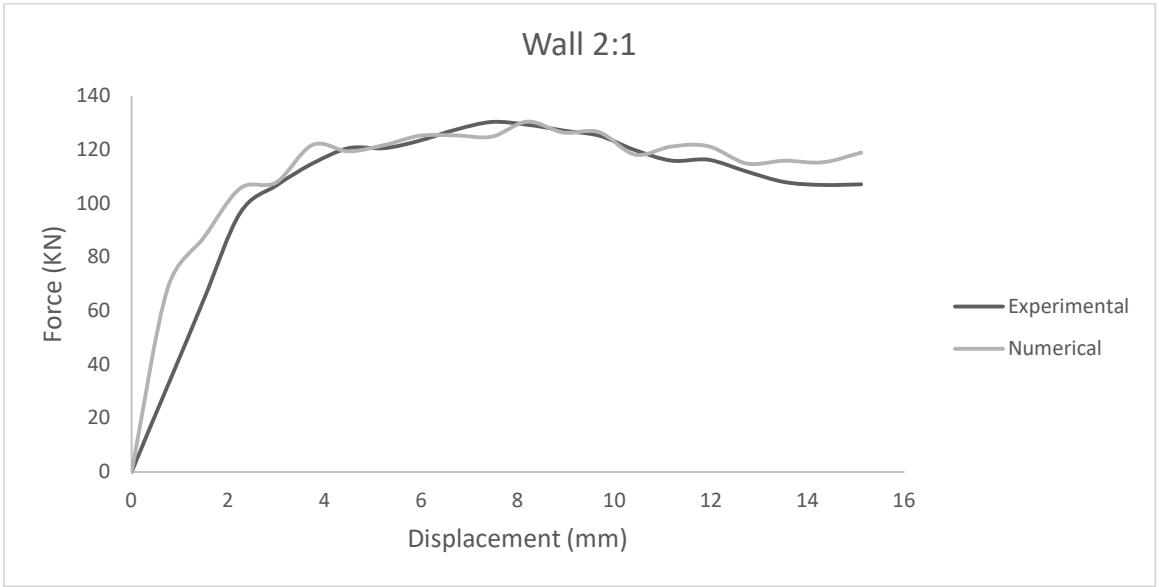

Figure 33: Wall 2:1 Experimental Vs Numerical Load Displacement Graph

Table 3: Experimental and Numerical Peak Strength Comparison

Wall Opening Aspect ratio	Experimental Results (KN)	ABAQUS FEA Results (KN)	Difference (KN) (%)
1:2	164.25	168.64	4.39(2.7)
1:1	153.71	155.40	1.69(1.1)
2:1	130.47	130.60	0.13(0.1)

Also, it has been noticed that crack pattern also matches to experimental.

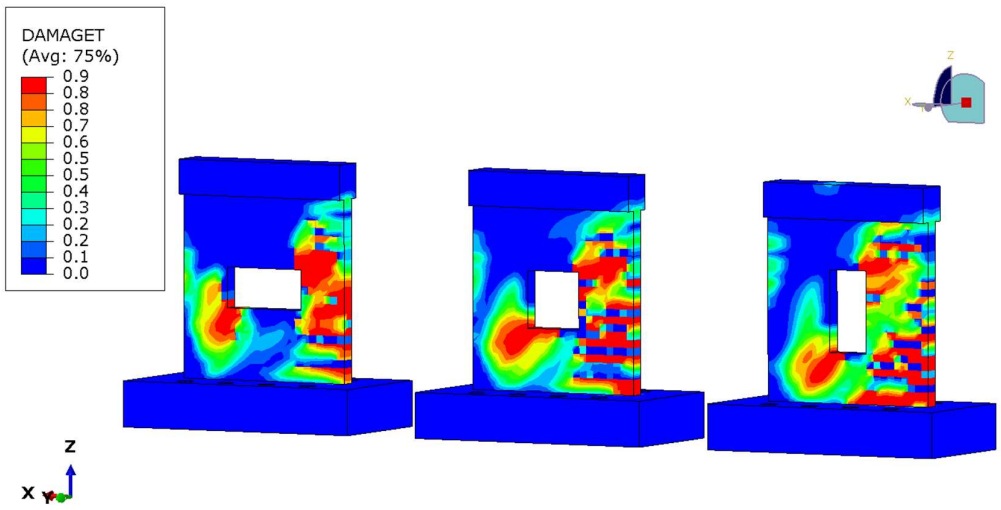

Figure 34: Tension Damage Parameter

Figure 35:Crack Patterns

Chapter-7

7 Conclusion:

Based on the comprehensive research conducted, several recommendations can be made regarding the aspect ratio of openings in squat walls. It is advisable, especially for utilities such as windows, to prefer openings with a low aspect ratio. This means that the height of the opening should be relatively smaller compared to its width. This recommendation is based on the findings that openings with a low aspect ratio have a lesser impact on the in-plane shear capacity of the shear wall or squat wall.

The experimental results clearly indicate that as the aspect ratio of the opening increases, the peak in-plane shear capacity of the wall decreases. This means that walls with larger openings or higher aspect ratios are more susceptible to shear failure and have a reduced load-carrying capacity. Therefore, to ensure the structural integrity and stability of the wall, it is preferable to choose openings with a lower aspect ratio.

Furthermore, the experimental results also show that the opening aspect ratio influences the stiffness of the wall. Although the effect is relatively small, it is still significant. As the aspect ratio decreases, the wall becomes stiffer, which is desirable in terms of structural performance and resisting deformations.

In addition to the shear capacity and stiffness, the aspect ratio of the opening also plays a role in the ductility of the wall against in-plane deformations. It was observed that each wall reached its peak load at different displacement values, indicating variations in ductility. Lower aspect ratios tend to enhance the ductility of the wall, allowing it to undergo larger deformations before reaching failure.

Therefore, considering the combined factors of shear capacity, stiffness, and ductility, it is recommended to select openings with a low aspect ratio for squat walls. This choice will help maintain the structural integrity, increase the load-carrying capacity, improve stiffness, and enhance the ductility of the wall.

8 Funding:

The research conducted for this study was solely funded by the researchers themselves, and no external agency or department funds were utilized. The researchers took personal responsibility for the financial aspects of the research, including the costs associated with materials, equipment, software, and any other expenses incurred during the study.

Chapter-8

9 References:

1. Gulec, C.K.; Whittaker, A.S.; Stojadinovic, B. Shear strength of squat rectangular reinforced concrete walls. *ACI Struct. J.* **2008**, *105*,488–497
2. Paulay, T.; Priestly, M.J.N. *Seismic Design of Reinforced Concrete and Masonry Buildings*; Wiley: New York, NY, USA, 1992
3. Kabeyasawa T, Kimura T. Ultimate strength reduction of reinforced concrete shear walls with an opening. Concr Eng Ann Meet 1989;11:585–90. [in Japanese].
4. Li Bing, Pan Z, Zhao Y. Seismic behaviour of lightly reinforced concrete structural walls with openings. Mag Concr Res 2015;67:843–54
5. Pilakoutas, K.; Elnashai, A.S. Cyclic Behavior of RC Cantilever Walls, Part I: Experimental Results. ACI Struct. J. 1995, 92, 271–281
6. Salonikios, T.N.; Kappos, A.J.; Tegos, I.A.; Penelis, G.G. Cyclic Load Behavior of Low-Slenderness Reinforced Concrete Walls: Design Basis and Test Results. ACI Struct. J. 1999, 96, 649–660.
7. Hidalgo, P.A.; Ledezma, C.A.; Jordan, R.M. Seismic Behavior of Squat Reinforced Concrete Shear Walls. Earthq. Spectra 2002, 18,287–308.
8. Salonikios, T.N. Shear strength and deformation patterns of R/C walls with aspect ratio 1.0 and 1.5 designed to Eurocode 8 (EC8).Eng. Struct. 2002, 24, 39–49
9. 6. Cheng, M.-Y.; Wibowo, L.S.B.; Giduquio, M.B.; Lequesne, R.D. Strength and Deformation of Reinforced Concrete Squat Walls with High-Strength Materials. ACI Struct. J. 2021, 118, 125–137.
10. An experimental investigation into the impacts of eccentric openings on the in-plane behavior of squat RC shear walls Seyed Armin Hosseinia,∗, Ali Kheyroddina, Mohammad Mastali

11. Ono M, Tokuhiro I. A proposal of reducing rate for strength due to opening effect of reinforced concrete framed shear walls. J Struct Constr Eng 1992:119–29. [in Japanese].
12. [4] Lin CY, Kuo CL. Behavior of shear wall with openings. Proceedings of ninth world conference on earthquake engineering, Tokyo-Kyoto, Japan, 4. 1988. p. 535–40
13. Massone Leonardo M, Munoz Gonzalo, Rojas Fabian. Experimental and numerical cyclic response of RC walls with openings. Eng Struct 2019;178:318–30
14. Johari, A., Pour, J., Javadi, A. (2015). Reliability Analysis Of Static Liquefaction Of Loose Sand Using the Random Finite Element Method. Engineering Computations, 7(32), 2100-2119. https://doi.org/10.1108/ec-07-2014-0152
15. Mao, R., Ye, X., Wang, H., Zhang, G., Wang, J. (2021). Magneto-induced Normal Stress Of Magnetorheological Gel Under Quasi-statically Monotonic and Periodically Cyclic Loading. Front. Mater., (8). https://doi.org/10.3389/fmats.2021.646579
16. Nie, S., Zhou, T., Zhang, Y., Zhang, B., Wang, S. (2020). Investigation On the Design Method Of Shear Strength And Lateral Stiffness Of The Cold-formed Steel Shear Wall. Mathematical Problems in Engineering, (2020), 1-13. https://doi.org/10.1155/2020/8959712
17. Xu, G., Li, A. (2018). Research On the Mechanical Characteristics And Calculation Method Of Concrete Cavity Shear Wall. Advances in Structural Engineering, 12(21), 1840-1852. https://doi.org/10.1177/1369433218757761
18. Yang, Y., Cao, W. (2016). Seismic Performance Of Shear Wall With Cfst Columns and Encased Steel Truss. Journal of Asian Architecture and Building Engineering, 3(15), 613-618. https://doi.org/10.3130/jaabe.15.613

19. Zhou, Y., Lu, X., Dong, Y. (2010). Seismic Behaviour Of Composite Shear Walls With Multi-embedded Steel Sections. Part I: Experiment. Struct. Design Tall Spec. Build., 6(19), 618-636. https://doi.org/10.1002/tal.597